Truncation Error Mitigation in Free-Space Automotive Partial Spherical Near Field Measurements

F. Saccardi, F. Rossi, L. Scialacqua, L. J. Foged
Microwave Vision Italy (MVI) SRL
Via dei Castelli Romani 59
00071 Pomezia, Italy
francesco.saccardi@microwavevision.com

***Abstract*— Antennas installed in modern cars are often highly integrated. In such cases, the entire vehicle is contributing to the radiated field, in particular at lower frequencies such as VHF. The complete characterization of the full vehicle is thus typically required. For frequencies down to 70 MHz, a widely accepted and cost effective solution is a multi-probe spherical Near Field (NF) system in which the scanning area is truncated below the horizon to minimize system dimensions. In order to emulate a proper free-space condition in the lower hemisphere, the ground floor is covered with absorbing material [1]. The partial NF acquisition of such systems leads to truncation errors if standard Near Field to Far Field (NF/FF) transformation is applied [2-3]. The mitigation of truncation error in general measurement scenarios by different post-processing techniques are described in the literature [4-9]. In this contribution, the mitigation capabilities of two techniques are investigated by experiment for an automotive scenario for the first time. The measurements have been performed on a 1:12 scaled vehicle-mounted antenna in a full-sphere multi-probe system. The scaled system and vehicle is representative of a real size system in the frequency range 70-400 MHz. Both truncated and full 3D measurements are performed for comparison.**

I. INTRODUCTION

In order to fully characterize the radiating properties of the vehicle mounted antennas, a large measurement system capable of accommodating the full vehicle is required. As in standard Near Field (NF) measurements, a full spherical scanning around the car is desirable in order to perform an accurate Near Field to Far Field (NF/FF) transformation. However, due to vehicle size, weight and/or economic factors, a full spherical scan is often unfeasible. For this reason, truncated spherical scanners are typically preferred. One solution is to combine hemispherical scanning with a metallic ground plane, assuming a Perfect Electric Conductor (PEC) in the NF/FF transformation [2-3]. However, PEC ground-planes are far from representative of realistic automotive environments such as asphalt that is strongly dielectric. A further drawback is the interaction of the large metallic ground-plane with the ambient structure, compromising the quality of the measurements. A much better approximation to realistic automotive environments is a condition similar to free-space using absorber materials on the floor [1]. An example of such system is shown in Figure 1.

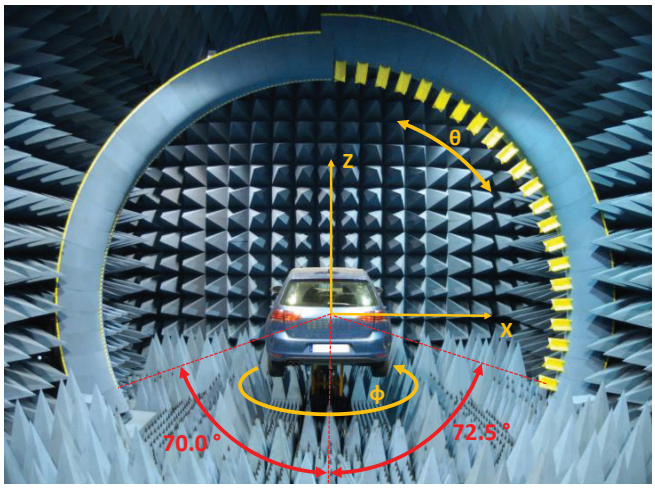

Figure 1. Multi-probe, Automotive Range at Ilmenau from MVG covering the 70 MHz to 6 GHz range.

Standard NF/FF transformations applied to partial spherical acquisitions generates truncation errors. Such errors are stronger at lower frequencies due to the lower number of spherical modes for fixed size Device Under test (DUT). Typical antennas for automotive applications are low directivity thus the impact of the truncation on the measured pattern is often non-negligible. In such cases, advanced post-processing techniques are employed to mitigate the effect of the truncation errors [4-9]. The effectiveness of these techniques is well documented for general NF antenna measurements. Two techniques have been selected for investigation for automotive applications. The first technique is an iterative process, combining Spherical Wave Expansion (SWE) and modal filtering [5-7]. The second technique is based on the EQuivalent Current (EQC) expansion [10-14]. EQC is a minimum energy operator, providing a smooth transition between the measured and truncated region.

In this paper, truncation errors mitigation in automotive testing scenarios are investigated experimentally.The DUT is a vehicle-mounted antenna in a 1:12 scale. Frequency scaled measurements are performed in a full-sphere multi-probe system giving access to both truncated and full 3D measurements of an equivalent system covering the 70-400 MHz range.

II. Truncation Errors in Free-Space Automotive Ranges

When the standard NF/FF transformation is applied to a truncated Spherical Near Field (SNF) dataset, the resulting FF pattern is generally affected by errors [4]. In this section, the effect of the truncation errors on a free-space automotive range is evaluated considering the measurement of a scaled car model.

A. Standard NF/FF transformation with Truncated SNF

Standard spherical NF/FF transformation is performed applying the so-called Spherical Wave Expansion (SWE) [3], where the measured field is projected over a set of orthogonal Spherical Wave Functions (SWF) computing the Spherical Wave Coefficients (SWC). It is well known that, in order to correctly perform the SWE, the input field must be defined over the full sphere. In case of field truncation, the missing portion of the sphere is typically filled with zeros (zero-padding) resulting in a discontinuous NF. In order to represent such a discontinuous field in the spherical wave domain, a very large number of SWF is needed (ideally an infinite number). Due to the cut-off properties of the SWE [3], the highest SWC order is given by

$$N_{max} = k\, R_{meas} = \frac{2\pi f}{c} R_{meas} \qquad (1)$$

where k is the wavenumber, c is the free-space speed of light, f is the frequency and R_{meas} is the radius of the measurement sphere. For a given and finite R_{meas}, the total number of computable spherical modes becomes bigger when the frequency is increased. Truncation errors are thus less important at higher frequencies because the discontinuity introduced by the zero-padding of the NF can be represented by a larger number of SWC.

B. Free-Space Automotive Scaled Measurement

An example of free-space automotive range [15-16] is shown in Figure 1. Such a system is the multi-probe automotive spherical NF system installed at the Ilmenau University and provided by Microwave Vision Group (MVG). The dimensioning of this automotive system have been taken into account in order to study the truncation errors in typical free-space automotive range.

As can be seem the ground floor is covered by absorbing materials, which reproduce the free-space condition. The systems is composed by two arrays of probes installed on an arch of 4-meter radius. The probe arrays allows for a fast electronic scanning in elevation. The probe array on the right is used to perform radiating measurements in the 70-400 MHz frequency range. To that end, 22 probes equally spaced in the $\theta = [2.5°, 107.5°]$ range are used. Instead, the probe array on the left is intended for measurements in the 0.4-6.0 GHz frequency range and is composed by 111 equally spaced probes in the $\theta = [0°, 110°]$ range. For both probe arrays, the φ-acquisition is performed by a turntable azimuthal rotation over full 360°. As illustrated in Figure 1, the resulting truncated areas are ±72.5° for the low frequency (LF) probe array and ±70.0° for the high frequency (HF) probe array.

In order to study the effect of the truncation in an automotive range similar to the one described above, a scaled car model has been measured in the MVG StarLab portable multi-probe system [17]. The StarLab has a measurement radius of 0.45 m and it is composed of two probe arrays able to perform measurement in the 0.65-6.00 GHz and 6.00-18.00 GHz frequency ranges, respectively.

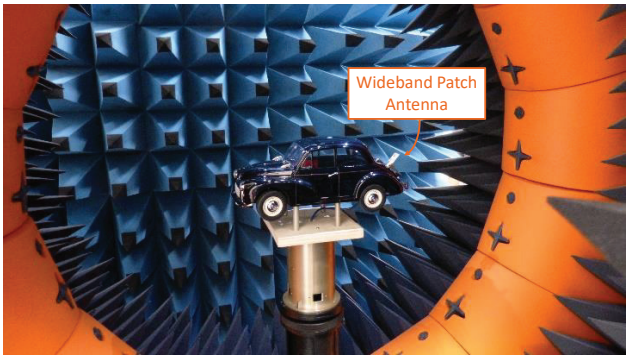

Figure 2. Measurement of the scaled car model in the MVG StarLab SNF system.

The car considered for the measurement is the 1:12 scaled model of the Morris Minor 1000 of 1965 shown in Figure 2. The dimensions of the scaled car are approximately: L x W x H = 31.3 x 12.9 x 12.7 cm (original dimensions: L x W x H = 3.76 x 1.55 x 1.52 m). A wideband patch antenna with omnidirectional pattern has been considered as AUT. The AUT has been installed on the rear hood of the car model as shown in Figure 2. The DUT (car model and patch antenna) has thus been measured in the MVG StarLab system (see Figure 2) at frequencies where the patch antenna has a good matching. The considered frequency range for the test is 1.1-18.0 GHz, approximately corresponding to the 91.7–1500.0 MHz scaled frequency range. The measurement setup of the performed StarLab measurement is summarized in the second column of Table I.

TABLE I. StarLab, Scaled and Equivalent Automotive Measurement Setup.

	StarLab Measurement	**Scaled StarLab Measurement**	**Equivalent Automotive Measurement**
Frequencies	(1.1–6.0 GHz)[a] (6.0–18.0 GHz)[b]	(1.1–4.8 GHz) (4.8–18.0 GHz)	(91.7-400.0 MHz)[c] (400.0-1500 MHz)[d]
Radius	(0.45 m)[a, b]	(0.33 m)	(4.00 m)[c, d]
Sampling	(Δθ = Δφ = 4.5°)[a] (Δθ = Δφ = 1.5°)[b]	(Δθ = Δφ = 5°) (Δθ = Δφ = 1°)	(Δθ = Δφ = 5°)[c] (Δθ = Δφ = 1°)[d]
Truncation	(±22.5°)[a, b]	(±72.5°) (±70.0°)	(±72.5°)[c] (±70.0°)[d]

[a] LF StarLab probe array, [b] HF StarLab probe array,

[c] LF automotive probe array, [d] HF automotive probe array

Reference FF data have been obtained applying the standard NF/FF transformation to the measured spherical NF neglecting the errors caused by the relative small truncation area of the StarLab systems (just ±22.5° in elevation).

The StarLab measurement has been scaled in order to reproduce the same conditions of a typical automotive system. In particular, a spherical back-propagation [3] to a measurement sphere of radius 0.33 m have been performed (the StarLab radius is 0.45 m while the needed scaled radius is 4/12 ~ 0.33 m). LF measurements have been emulated by taking into account the data in the 1.1-4.8 GHz frequency range and reproducing the ±72.5° truncated area. HF measurements have instead been emulated considering the NF data in the 4.8-18.0 GHz frequency range and reproducing the ±70.0° truncated area. For LF and HF probe arrays, also the same condition of the real automotive range in terms of sampling has been considered: $\Delta\theta = \Delta\varphi = 5°$ for the LF probe array and $\Delta\theta = \Delta\varphi = 1°$ for the HF probe array. The parameters of the scaled StarLab measurement are summarized in the third column of Table I. The results obtained by processing such a scaled measurement are directly applicable to the equivalent automotive measurement summarized in the last column of Table I.

The scaled measurements have been processed with the standard NF/FF transformation performing a zero-padding in the truncated area. In order to evaluate the loss of accuracy due to the truncation, the FF obtained from the scaled automotive measurement has been compared with the reference FF. To do that, the Equivalent Noise Level (ENL) defined by the following formula has been used

$$ENL = 20\log_{10}\left(mean\left|\frac{E(\theta,\varphi) - \tilde{E}(\theta,\varphi)}{E(\theta,\varphi)_{MAX}}\right|\right) \qquad (2)$$

where $E(\theta,\varphi)$ is the reference FF pattern and $\tilde{E}(\theta,\varphi)$ is the test FF pattern. The ENL has been evaluated only on the measured portion of the sphere. The ENL at each (scaled) frequency is shown in Figure 3 for both the LF and HF probe arrays. The truncation errors are definitely higher at LF (up to 400 MHz) where, as explained above, the number of SWC used to represent the scenario is smaller. On the other hand, the truncation errors can be considered negligible at HF (above 400 MHz) where the higher sample density allows to compute more SWC and thus to better represent the introduced discontinuity.

In order to reduce the truncation errors at lower frequencies, two advanced post-processing techniques have been applied to the scaled LF measurement in the 91.7–400.0 MHz frequency range, where the ENL is above -35 dB.

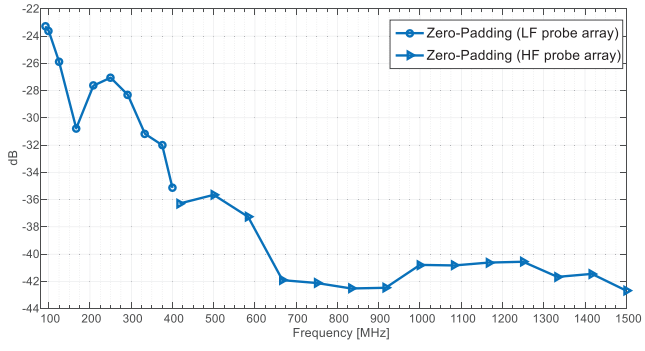

Figure 3. ENL with frequency in typical automotive measurements using zero-padding.

III. Advanced Post-Processing Techniques

The two advanced post-processing techniques considered in this paper for the mitigation of the truncation errors are:

- Iterative modal filtering (IMF)
- EQuivalent Currents (EQC)

A brief description of the two techniques is reported in this section.

A. *Iterative Modal Filtering*

The iterative modal filtering (IMF) has already been presented in previous papers [5-7]. It is based on the SWE and modal filtering of the measured field, which are repeated iteratively. The workflow of the IMF is shown in Figure 4.

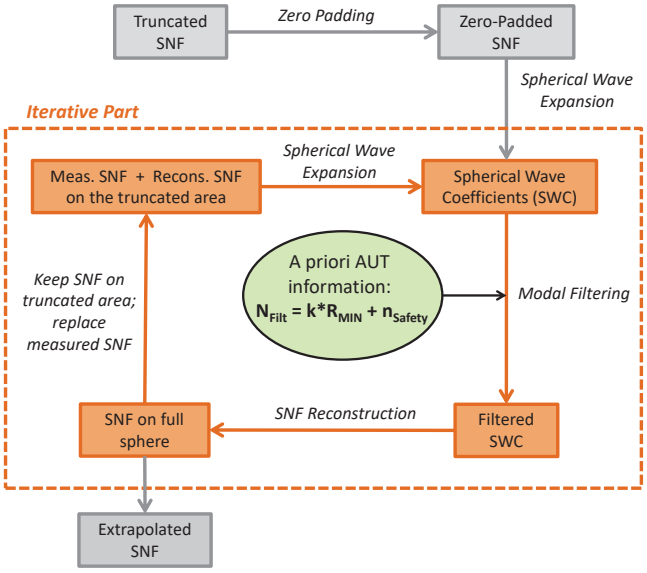

Figure 4. Block diagram of the IMF technique.

As can be seen, the truncated area of the measured SNF is first filled with zeros (zero-padding) and is expanded in terms of spherical waves (SWE) obtaining the SWC. The SWC are then filtered on the base the DUT physical dimensions. More specifically, it is known that a DUT can be fully represented in the spherical wave domain with the following number of spherical radial modes

$$N_0 = k\,R_{min} + n_1 \qquad (3)$$

where R_{min} is the radius of minimum sphere enclosing the DUT [3] and n_1 an integer number used as "safety" margin [3]. In ideal conditions, SWC having radial indices bigger than N_0 are expected to be negligible. Instead, when the SWC are calculated from a zero-padded truncated SNF, coefficients corresponding to indexes higher than N_0 may have non-negligible amplitude. A low pass modal filtering is thus applied at $N_{filt} = N_0$, in order to partially remove the effect of the truncation.

From the filtered SWC, the SNF at the same measurement radius is computed on the full sphere. The computed NF samples in the truncated region are an improved estimate of the missing samples. In the last step of the procedure, these extrapolated samples are thus kept while the recomputed NF samples on the un-truncated region are replaced with the real measured data, being not affected by errors due to the truncation.

This process is repeated until the convergence is reached. It is specified that the convergence of the algorithm can be controlled by computing at each iteration the ENL (see equation 2) between measured and reconstructed samples in the un-truncated region. When a certain threshold level defined by the user is reached, the iterative process is terminated.

B. *Equivalent Currents (INSIGHT)*

Starting from the measured NF or FF data, the EQuivalent Currents (EQC) technique allows to compute equivalent electric and magnetic radiating currents on an arbitrary shaped reconstruction surface fully enclosing the test object. The EQC technique is implemented in the commercially available MVG INSIGHT software [18] and it can be used for many post-processing purposes including diagnostic [10-11], spatial filtering [12-13], source for numerical computation [14] and NF/FF transformation for both complete and truncated NF data set [7, 19].

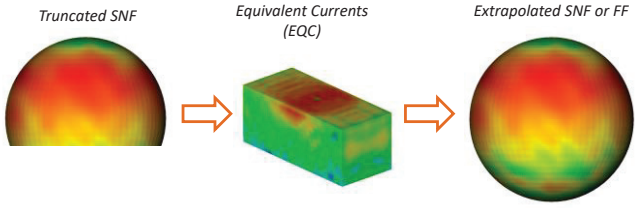

Figure 5. Block diagram of the EQC technique used as tool for mitigation of truncation errors.

A simple block diagram regarding the use of the EQC as NF/FF transformation tool for truncated SNF dataset is reported in Figure 5. As can be seen, the truncated SNF dataset is directly used without performing any field padding (as done in the IMF technique) which would result in a discontinuous and un-physical field. The EQC computation is in fact a minimum energy operator on the truncated region, which allows for a direct computation of the currents avoiding errors caused by the processing of a discontinuous field. From the computed EQC the FF is finally evaluated over the full sphere completing the NF/FF transformation process. Alternatively, it also possible to re-compute the NF on the spherical surface and then apply the standard NF/FF transformation. For the sake of simplicity, the first possibility has been adopted in this work.

IV. Reduction of Truncation Errors at Low Frequencies

The two advanced post-processing techniques for the mitigation of the truncation errors have been applied to the measurement of the scaled car where the same measurement conditions of the Ilmenau automotive range have been reproduced. As previously pointed out, frequencies corresponding to the LF probe array are the most sensible to the truncation of scanning area. Thus, the analysis has been carried out only the 91.7-400.0 MHz frequency range.

The IMF technique has been applied considering a radius of the DUT minimum sphere of 20 cm (minimum sphere of the scaled vehicle) and performing 603 iterations (ENL near field threshold level set to -60 dB).

The EQC technique have instead been applied considering an equivalent box for the current reconstruction of size: L x W x H = 35 x 20 x 18 cm, fully enclosing the scaled vehicle. The equivalent box has been discretized with a mesh made of triangles with side length λ/4. It should be noted that the number of unknowns increases with the frequency leading to different computational effort at the considered frequencies (see Table II).

The substitution (or gain transfer) technique [2], has been adopted in order to compute the gain of the DUT. To that end, the measurement system has been properly calibrated using a reference gain antenna. Each pattern comparison that will be shown in the following is thus gain normalized.

The comparison in terms of ENL between: FF obtained with zero-padding (blue trace), IMF technique (orange trace) and EQC/INSIGHT technique (green trace) is reported in Figure 6. The ENL formula has been applied considering only the portion of the FF radiation pattern corresponding to the un-truncated region (reliable part of the sphere, $\theta_{max} = 107.5°$). As can be seen, both post-processing techniques are able to improve the gain radiation pattern obtained with the simple zero-padding of the truncated area. It is clear that the achieved performance of the EQC are better with respect to the IMF at almost each test frequency. In particular, at frequencies up to approx. 170 MHz, the relative high ENL obtained with the zero-padding are lowered of 7.5-10 dB with the EQC, while the IMF is capable to give only 1.5-4 dB of improvement. In the central part of the band, the improvements obtained with EQC are very good, being around 10 dB, and those obtained with the IMF approximately 5-6 dB. In the high end of the bandwidth, the two techniques have similar behaviors (5-6 dB of improvement with respected to the zero-padding).

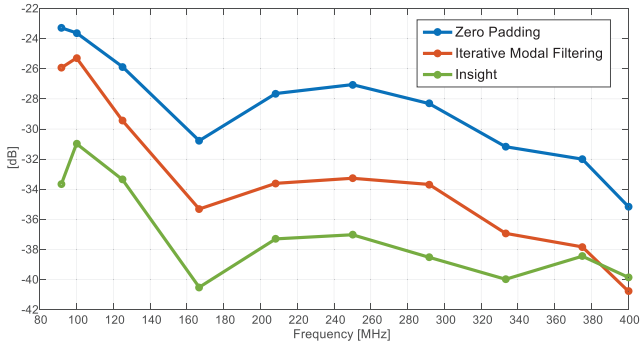

Figure 6. ENL with frequency obtained with the different techniques.

Gain radiation pattern comparison at 91.7 MHz, are reported in Figure 7 and Figure 8 respectively for the vertical cut at φ=0° and for the horizontal cut at θ=90°. The reported traces are the total field cuts of the reference pattern (black trace), pattern obtained with zero-padding (blue trace), IMF technique (orange trace) and EQC technique (green trace). The shadowed areas drawn in the vertical cut illustrate the truncated and thus unreliable regions. The perturbation introduced by the truncation of the scanning area is observable in the zero-padded pattern in both presented cuts. It is stressed that the truncation errors are not just present in the unreliable region, but all over the pattern. The improvements obtained with the EQC technique are clearly observable in the reliable region of the vertical cut shown in Figure 7. Instead, as previously observed in the ENL comparison, the performance of the IMF technique are worse at this test frequency. A similar comment can be applied also to the horizontal cut shown in Figure 8 where the EQC technique gives a very good agreement with the reference

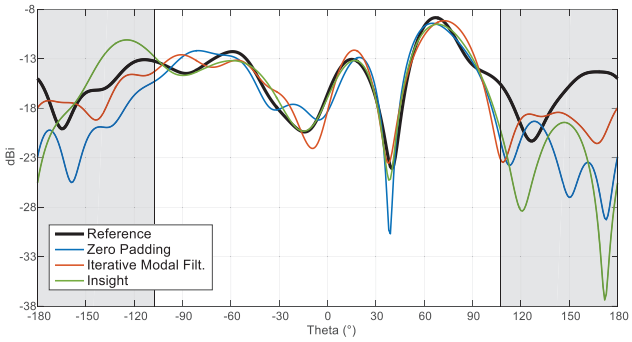

Figure 7. Gain pattern comparison at 91.7 MHz; vertical cut at φ = 0°.

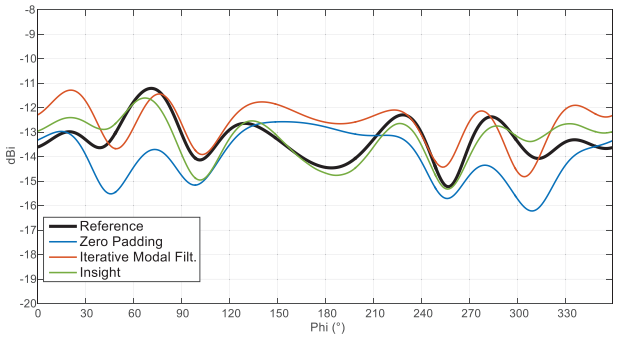

Figure 8. Gain pattern comparison at 91.7 MHz; horizontal cut at θ = 90°.

Gain pattern comparisons similar to the previous ones are reported in Figure 9 and Figure 10 for the test frequency of 250 MHz. Even in this case, the truncation effect is visible all over the zero-padded pattern cuts. The improvements obtained with the two techniques are remarkable and very similar in the -70°< θ <+80° angular range of the vertical cut shown in Figure 9. In the same cut, it is observed that the EQC technique is able to give better performance at θ-values close to the truncation. The high performance of the two techniques are also remarked in the horizontal cut shown in Figure 10, where they both give good and similar results.

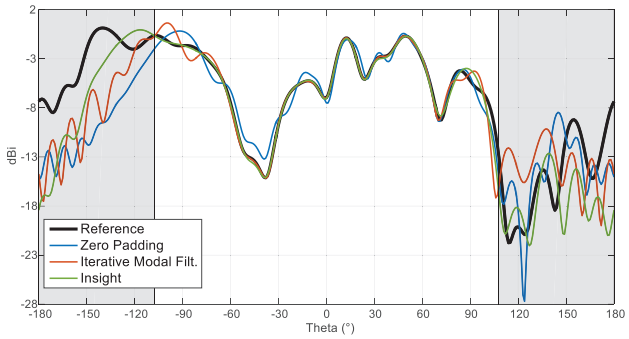

Figure 9. Gain pattern comparison at 250 MHz; vertical cut at φ = 0°.

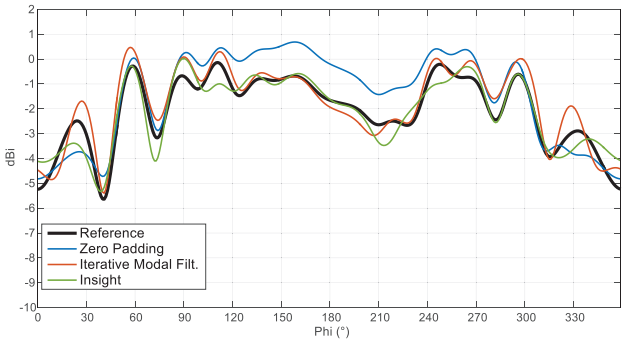

Figure 10. Gain pattern comparison at 250 MHz; horizontal cut at θ = 90°.

The computational times of the EQC and IMF technique, both obtained with the same standard laptop computer, are shown in Table II. The complete IMF multi-frequency processing (10 frequencies in total) run in approximately 90 seconds. As can be seen, the EQC running time increases with frequency leading a much more demanding total process with respect to the IMF technique.

TABLE II. COMPUTATIONAL TIME OF THE EQC AND IMF TECHNIQUE.

Frequency (MHz)	**EQC**	**IMF**
91.7	~ 8 s	~ 90 s
100.0	~ 9 s	
125.0	~ 18 s	
166.7	~ 37 s	
208.3	~ 75 s	
250.0	~ 126 s	
291.7	~ 162 s	
333.3	~ 224 s	
375.0	~ 343 s	
400.0	~ 376 s	
Total	**~ 23 min**	**~ 1.5 min**

V. CONCLUSIONS

Two advanced post-processing techniques for the mitigation of the truncation errors, the EQuivalent Currents (EQC) and the Iterative Modal Filtering (IMF), have been applied to the measurement of a 1:12 scaled vehicle performed in a MVG StarLab multi-probe system. The considered test case is intended to emulate a realistic multi-probe automotive measurement scenario performed in free-space conditions and a having large truncated area (approximately ±70° in elevation).

The truncation errors in case of standard NF/FF transformation (performed by simply setting to zero the missing sample points) have been first analyzed in the 91.7–1500.0 MHz frequency range. As expected, it has been shown that, due to the lower number of spherical modes for fixed DUT size, the effect of the truncation is much more important at lower frequencies. The analysis has thus been limited to the 91.7–400.0 MHz frequency range, which, in a typical MVG multi-probe automotive measurement scenario, can be measured by the low frequency probe array spanning from 70 MHz to 400 MHz.

Application of both advanced post-processing techniques to the scaled automotive measurement has shown significant improvements with respect to the standard approach. The computational cost of the EQC increases with the frequency and is in general much higher with respect to the IMF. The EQC has shown better performance with respect to the IMF at lower frequencies, where its computational cost it not very high. The achieved performance of two techniques are instead very similar at higher frequencies where is thus convenient to use the IMF being much faster.

REFERENCES

[1] P. Noren, Ph. Garreau, L. J. Foged, "State of the art spherical near-field antenna test systems for full vehicle testing, EuCAP, March 2012, Prague, Czech Republic

[2] IEEE Std 1720-2012 "Recommended Practice for Near-Field Antenna Measurements"

[3] J. E. Hansen (ed.), Spherical Near-Field Antenna Measurements, Peter Peregrinus Ltd., on behalf of IEE, London, United Kingdom, 1988

[4] L. J. Foged, L. Duchesne, Ph. Garreau, P.O. Iversen, J-Ch. Bolomey, "Truncation impact on measured radiation pattern in spherical near field antenna test ranges", IEEE APS Symposium and USNC-URSI National Radio Science Meeting, July 8-12, 2001, Boston, USA.

[5] E. Martini, S. Maci, L. J. Foged, "Spherical Near Field Measurements with Truncated Scan Area", 5th European Conference on Antennas and Propagation, EuCAP 2011, Rome, Italy, 11-15 April 2011.

[6] E. Martini, S. Maci, L. J. Foged, "Reduction of Truncation Errors in Spherical Near Field Measurements", AMTA 2010, 10-15 October, Atlanta, Georgia, USA

[7] L.J. Foged, L. Scialacqua, F. Saccardi, F. Mioc, J. L. Araque Quijano, E. Martini, S. Maci, M. Sabbadini, G. Vecchi, "Comparative Investigation of Methods to Reduce Truncation Errors in Partial Spherical Near-Field Antenna Measurements" EuCAP 2012, 26-30 March, Prague, Czech Republic

[8] Ronald C. Wittmann, Carl F. Stubenrauch and Michael H. Francis "Using Truncated Data Sets in Spherical Scanning Antenna Measurements" International Journal of Antennas and Propagation, Volume 2012 (2012)

[9] Francisco José Cano-Fácila, Sergey Pivnenko, and Manuel Sierra-Castañer, "Reduction of Truncation Errors in Planar, Cylindrical and Partial Spherical Near-Field Antenna Measurements" International Journal of Antennas and Propagation, Volume 2012 (2012)

[10] J. L. Araque Quijano, G. Vecchi. Improved accuracy source reconstruction on arbitrary 3-D surfaces. Antennas and Wireless Propagation Letters, IEEE, 8:1046–1049, 2009.

[11] L. Scialacqua, F. Saccardi, L. J. Foged, J. L. Araque Quijano, G. Vecchi, M. Sabbadini, "Practical Application of the Equivalent Source Method as an Antenna Diagnostics Tool", AMTA Symposium, October 2011, Englewood, Colorado, USA

[12] L. J. Foged, L. Scialacqua, F. Mioc,F. Saccardi, P. O. Iversen, L. Shmidov, R. Braun, J. L. Araque Quijano, G. Vecchi" Echo Suppresion by Spatial Filtering Techniques in Advanced Planar and Spherical NF Antenna Measurements ", AMTA, Oct 2012, Seattle, Washington, USA

[13] J. L. A. Quijano, G. Vecchi, L. Li, M. Sabbadini, L. Scialacqua, B. Bencivenga, F. Mioc, L. J. Foged "3D spatial filtering applications in spherical near field antenna measurements", AMTA 2010 Symposium, October, Atlanta, Georgia, USA.

[14] L. Scialacqua, L. J. Foged, F. Mioc, F. Saccardi, "Link Between Measurement and Simulation Applied to Antenna Scattering and Placement Problems", EuCAP 2017, 19-24 March, Paris, France

[15] MVG automotive range website: "http://www.mvg-world.com/en/products/field_product_family/antenna-measurement-2/sg-3000f"

[16] MVG automotive range website: http://www.mvg-world.com/en/products/field_product_family/antenna-measurement-2/sg-3000-m

[17] MVG StarLab website: http://www.mvg-world.com/en/products/field_product_family/antenna-measurement-2/starlab

[18] MVG Insight website: "http://www.mvg-world.com/products/field_product_family/antenna-measurement-2/insight"

[19] Andrea Di Cintio, Giuliano Della Pietra, Alberto Caliumi, Gianpiero Duchini, Lars Jacob Foged, Andrea Giacomini, Francesco Saccardi, Luca Maria Tancioni, Nelson J. G. Fonseca "Measurement of Embedded Array Elements of VHF Satellite in Hemispherical NF Antenna Test Range"35th ESA WORKSHOP, 10-13 September 2013, ESA/ESTEC, Noordwijk, The Netherlands